  Bull. Chem. Soc. Jpn., 59, 133—137 (1986)

Thermal Stability of Electroless Nickel-Molybdenum-Phosphorus Alloy Films

Ichiro KOIWA, Masao NISHIKAWA, Keizo YAMADA, and Tetsuya OSAKA*
Department of Applied Chemistry, School of Science and Engineering,
Waseda University, Okubo, Shinjuku-ku, Tokyo 160
(Received July 12, 1985)

The structure and the electric resistivity of electroless Ni–Mo–P alloy films, which were plated from a caustic alkali citrate-glycolic acid bath, have been investigated. The phosphorus content in deposits and the deposition rate decreased with increasing Mo-complex concentration which was formed with sodium gluconate before constructing the bath. The crystallized structure and the formation of solid solutions between the Ni matrix and the codeposited Mo were indicated by X-ray diffraction measurments for high Mo-complex concentration range. On the other hand, amorphous states appeared for the Mo-complex concentration range lower than 0.002 mol dm^{-3}. In the range less than 0.002 mol dm^{-3} Mo-complex concentration, the resistivity of as-plated Ni–Mo–P films was higher than the binary Ni–P alloy film plated from the bath without the Mo-complex. In the higher Mo-complex concentration range, the resistivity immediately reached a constant value independently of the Mo-complex concentration. After 500 and 800 °C heat treatment under vacuum, the resistivity increased with increasing Mo-complex concentration. Moreover for the higher Mo-complex concentration range, the resistivity after heat treatment became higher than that of as-plated conditions, and the increased resistivity after the heat treatment depended on the Mo content in the deposits. Therefore, the codeposited Mo tended to increase the thermal stability of the films.

Recently, some workers applied electroless Ni–P plating films to thin film resistors[1,2] taking into account some advantages of mass production capability and good cost performance as compared with those prepared by PVD[3] and thick film[4] technologies. Since the amorphous Ni–P alloy film with high phosphorus content, easily produced by electroless plating method,[5,6] has high specific resistance and low temperature coefficient of resistivity,[7] it has been applied to the fields.

The structure of electroless Ni–P films[5,6,8–12] and the structure variation by heat treatment[13–15] have been studied, but satisfactorily thermally-stabilized amorphous Ni–P films have not been reported.

It is important to improve the thermal stability of electroless Ni–P plating films in view of their application to thin-film resistors. The codeposition of a higher-melting-metal into the Ni–P film is one of the candidates to improve the thermal stability of electroless Ni alloy films. Ternary alloy films of electroless Ni–W–P[16,17] and Ni–Mo–P[18,19] have already been reported. Their thermal variation is different from that of binary Ni–P alloy films, however, the study from this viewpoint has scarcely been reported and the thermal stability of the resistivity of the ternary alloy has not been discussed in detail.

This paper describes the correlation between the structure and the electric resistivity of electroless Ni–Mo–P alloy films and discusses the effect of molybdenum codeposition into Ni–P films.

Experimental

Electroless nickel–molybdenum–phosphorus alloy films were plated from a caustic alkali citrate–glycolic acid bath whose compositions and operating conditions were listed in Table 1. Molybdenum codeposition was easily formed by complexing sodium molybdate with sodium gluconate before constructing the bath as an analogy to the method by Mallory.[20] The solution of sodium molybdate which is complexed with sodium gluconate is designated Mo-complex in the text. The ninety-six w/o α-alumina ceramics (NGK Spark Plug Co. Ltd.) were used as a plating substrate except for the differential scanning calorimetry (DSC) measurement. For the DSC measurement, the catalyzed polyimide film (25KA, Torey Co. Ltd.) was used as substrate. The repeated two step process[21] was used for catalyzing the ceramics substrate, where the sensitizer and the activator are as follows; sensitizer: $SnCl_2 \cdot 2H_2O$ 1.0 g dm^{-3}, 37% HCl 1.0 ml dm^{-3}, and activator: $PdCl_2$ 0.1 g dm^{-3}, 37% HCl 0.1 ml dm^{-3}. The film thickness was adjusted to 2 μm by controlling the deposition time. The molybdenum and phosphorus contents shown as weight percentage (wt%) were determined by an inductively coupled argon plasma atomic emission spectrophotometer (ICAP-575 MarkII, Nippon Jarrell-Ash). The resistivity of the deposits on the alumina substrate was measured by the four-probe method. The structure of the deposits was determined using an X-ray diffractometer (RAD-IIA, Rigaku Denki Co. Ltd.). Thermal analysis was made with DSC (DSC-30, Shimadzu Co. Ltd.). The samples were prepared by grinding the deposits which were peeled off the polyimide substrate. The samples were heated from room temperature up to 500 °C at a constant rate of 10 °C/min, in a nitrogen atmosphere, using 10—20 mg

Table 1. Electroless Plating Bath Compositions and Operating Conditions

Chemicals	Concentration
$NaH_2PO_2 \cdot H_2O$	0.20 mol dm^{-3}
$C_3H_4(OH)(COONa)_3 \cdot 2H_2O$	0.10
$HOCH_2COOH$	0.20
$NiSO_4 \cdot 7H_2O$	0.10
Mo-complex	0—0.015

Bath temperature 90 °C, Bath pH 9.0 adjusted by NaOH.

sample weight. The heat treatment of the deposits was made under 2×10^{-3} Pa with 10 °C/min constant heating rate from room temperature to the setting temperature afterward the sample was maintained for one hour at the setting temperature.

Results and Discussion

Deposition Rate and Film Composition of Electroless Ni-Mo-P Alloy Films. The deposition rate and film composition at various Mo-complex concentration are shown in Fig. 1. The molybdenum content in the deposits increases with increasing the Mo-complex concentration up to 0.01 mol dm^{-3}, then it reaches a constant value. The maximum Mo content, 16.8 wt%, was obtained at 0.015 mol dm^{-3} Mo-complex concentration. The deposition rate decreases with increasing Mo-complex concentration and finally no deposition occurs at the region more than 0.015 mol dm^{-3} Mo-complex concentration. In contrast to Mo content behavior, the phosphorus content decreases with increasing the Mo-complex concentration. In particular, the phosphorus content remarkably decreases until 0.0025 mol dm^{-3} Mo-complex concentration, and the phosphorus content is depressed under 2 wt% at the region more than 0.0025 mol dm^{-3} Mo-complex concentration.

Structure and Resistivity of Electroless Ni-Mo-P Alloy Films. Figure 2 shows typical X-ray diffraction patterns of the deposits at various Mo-complex concentrations in the bath. As is seen in Fig. 2, the structure of the Ni-P alloy film without Mo-complex addition is in an amorphous state; only two peaks appear due to the Al_2O_3 substrate. In the region below 0.002 mol dm^{-3}, the structure of the Ni-Mo-P alloy films is in the same amorphous state as that of the Ni-P alloy film. On the other hand, at the region more than 0.002 mol dm^{-3} Mo-complex concentration, the structure of the Ni-Mo-P alloy films changes to a crystallized state. The structural change can be due to the remarkable decrease of the P content, as is seen in Fig. 1. Since the peaks of the Ni(111) and Ni(200) planes shift to the lower angle side as compared with the pure Ni value, the interplanar spacing of the Ni-Mo-P alloy can be widened by the molybdenum codeposition. The specific resistance, ρ, and the interplanar spacing, d, of Ni-Mo-P alloys are shown in Fig. 3 as a function of Mo-complex concentration. The ρ value increases with Mo-complex concentration up to 0.001 mol dm^{-3}, and it decreases to 0.0025 mol dm^{-3}. However, the ρ value becomes constant at 100 $\mu\Omega$ cm in the crystallized region above 0.0025 mol dm^{-3}. The d value of the crystallized Ni-Mo-P alloy films increases with increasing Mo-complex concentration. The increase in d value in the crystallized states

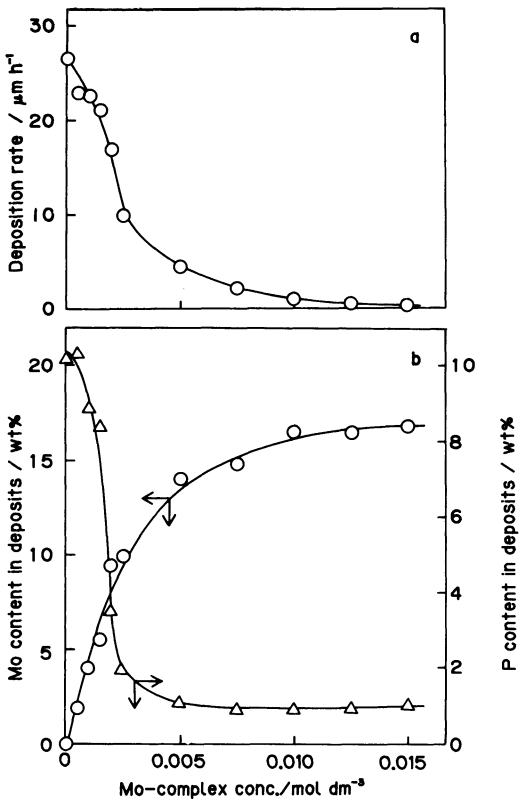

Fig. 1. Effect of Mo-complex concentration on deposition rate and film composition.

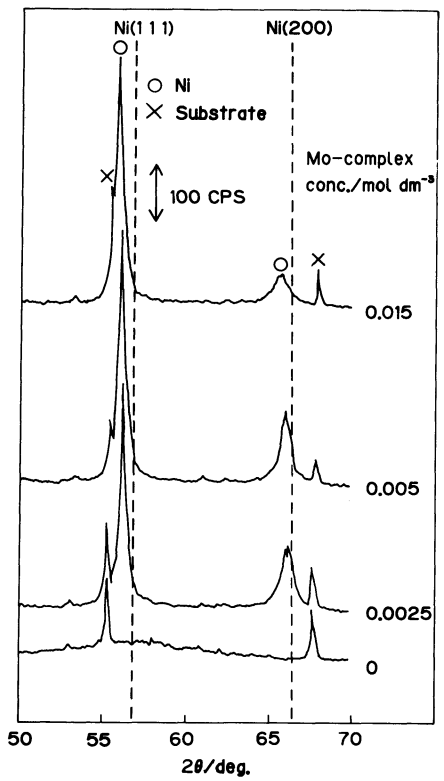

Fig. 2. X-Ray diffraction patterns for Ni-Mo-P alloy films with various Mo-complex concentrations using Fe target. Dashed lines show the peak positions of pure Ni.

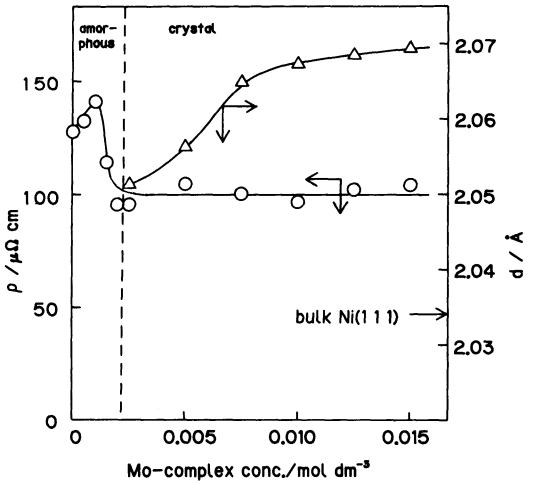

Fig. 3. Effect of Mo-complex concentration on specific resistance (ρ) and interplanar spacing (d) of Ni–Mo–P alloy films. Dashed line shows the phase change from amorphous to crystallized states.

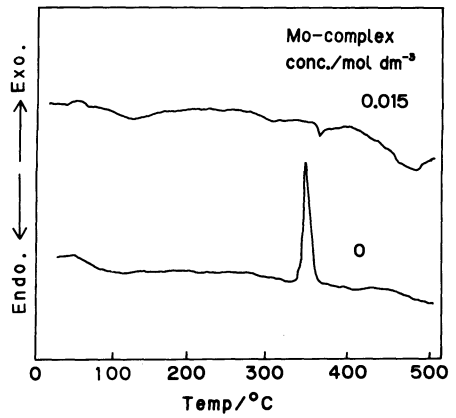

Fig. 4. DSC curves of Ni–P and Ni–Mo–P films.

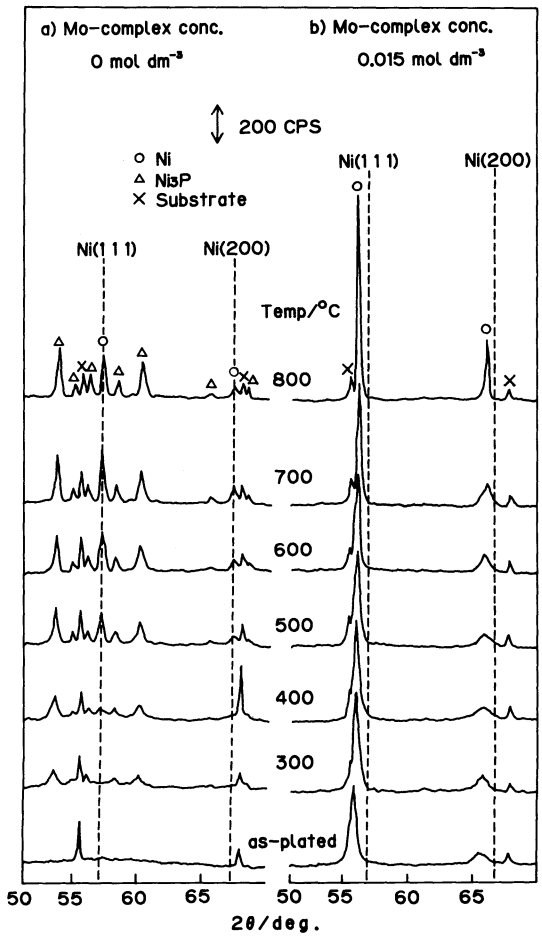

Fig. 5. X-Ray diffraction patterns for Ni–P and Ni–Mo–P alloy films at various annealing temperatures. Dashed lines show the peak positions of pure Ni.

corresponds to the increase in the Mo content with increasing Mo-complex concentration, but the ρ value of the films is independent of the increase in the Mo content. When considering that the ρ value of crystallized Ni–P alloy films with low phosphorus content generally becomes much lower than that of amorphous films,[22] the molybdenum codeposition into the Ni–P film might form a solid solution with a nickel matrix which results in the higher ρ value, in spite of the very low P content. The resistivity of as-plated Ni–Mo–P films, however, have no clear correlation with the Mo content.

Differential Scanning Calorimetry (DSC) Measurements. The DSC curves clearly show the difference between Ni–P and Ni–Mo–P deposits as is seen in Fig. 4. In the case of Ni–P film, there appears one clear exothermic peak around 350 °C, which coincides well with the previous studies.[13–15] In contrast to that of the Ni–P film, there is no obvious peak for Ni–Mo–P alloy films. In general, the exothermic peak is related to a structural change which affects the film properties such as the resistivity, and the magnetic and mechanical properties.[13–16] Therefore, the structure of an electroless Ni–Mo–P alloy film can be thermally more stable than that of a Ni–P alloy film.

Heat Treatment Effects on Properties of Electroless Ni–Mo–P Alloy Films. Figure 5 demonstrates typical X-ray diffraction patterns of the electroless Ni–P and the Ni–Mo–P alloy films after heat treatment at various temperatures. The amorphous Ni–P alloy film changes to a crystalline state and forms a Ni_3P compound on heat treatment at 300 °C. The structural change corresponds to the exothermic peak of the DSC curves as is seen in Fig. 4. The peak intensities of the Ni and Ni_3P increase with increasing heat treatment temperature. On the other hand, the electroless Ni–Mo–P alloy film, which has a crystalline structure at the as-plated conditions, maintains almost the same structure as that of an as-plated film up to 300 °C heat treatment. Moreover the peak intensities of the Ni(111) and Ni(200) plane gradually increase with the increase in the heat treatment temperature more than 300 °C. Therefore,

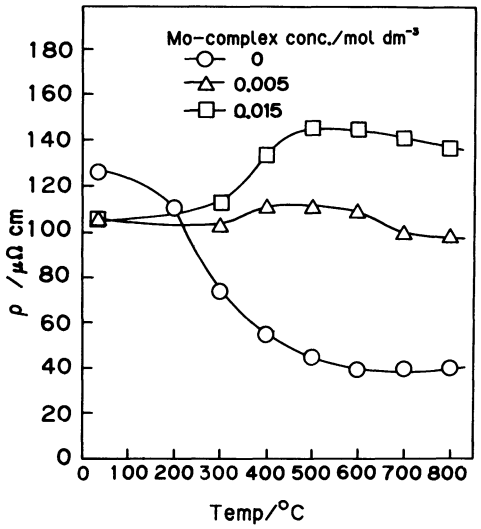

Fig. 6. Variation of specific resistance, ρ after heat treatment.

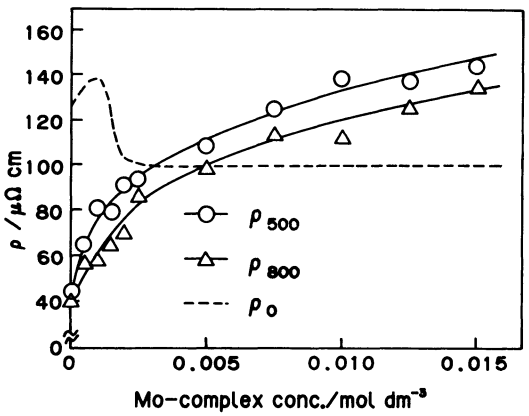

Fig. 7. Effect of Mo-complex concentration on resistivity after 500 and 800 °C heat treatment. Dashed line shows the resistivity, ρ_0 at as-plated conditions.

crystallization of electroless Ni–Mo–P alloy films is gradually proceeded by heat treatment. However, crystallization of Ni–Mo–P alloy film is much less than that of Ni–P alloy films, as has been reported previously.[13–15] The other peaks except for Ni(111) and Ni(200) planes are not observed for thermally-treated Ni–Mo–P films. The results coincide well with DSC measurement as is seen in Fig. 4. The molybdenum codeposition might inhibit the crystallization of a Ni matrix in contrast to the general Ni–P film with low phosphorus content.

Figure 6 illustrates the effect of heat treatment on the specific resistance (ρ) of Ni–Mo–P films. As is seen in Fig. 6, the resistivity of a Ni–P alloy film decreases remarkably with increasing heat treatment temperature. The decrease of Ni–P film resistivity starts in the lower heat treatment temperature range, and the decreased amount becomes larger with the increase in setting temperature. The results for a Ni–P film correspond well to those of the X-ray analysis as is shown in Fig. 5. On the other hand, the ρ value variation of electroless Ni–Mo–P alloy films is quite different from that of Ni–P alloy films, i.e., the ρ value variation is much smaller than that of a Ni–P alloy film. The resistivity of a Ni–Mo–P alloy film deposited from 0.005 mol dm^{-3} Mo-complex concentration bath is almost independent of the heat treatment temperature. Moreover, the resistivity of a Ni–Mo–P alloy film deposited from 0.015 mol dm^{-3} Mo-complex concentration bath increases with the heat treatment temperature and reaches a maximum around 500—600 °C. Such a tendency has not been observed for the binary electroless Ni–P and Ni–B alloy films. It can be concluded that the molybdenum codeposited into Ni–P film gives high stability against thermal treatment, and moreover that the Ni–Mo–P film of the higher Mo content shows the higher resistivity than that of as-plated one after heat treatment.

Figure 7 demonstrates the ρ value variation of Ni–Mo–P alloy films after heat treatment as a function of Mo-complex concentration. The resistivities after 500 °C and 800 °C heat treatments are denoted as ρ_{500} and ρ_{800}, respectively, and the dashed line indicates the resistivity value ρ_0 at as-plated conditions. The dashed line crosses solid lines of ρ_{500} and ρ_{800} values at 0.0035 and 0.005 mol dm^{-3} Mo-complex concentrations, respectively. It means that the ρ_{500} and ρ_{800} values become higher than the ρ_0 value at the region more than 0.0035 mol dm^{-3} and 0.005 mol dm^{-3} Mo-complex concentrations, respectively. The small difference of the degree of Ni matrix crystallization between 500 and 800 °C heat treatment can be observed as is seen in Fig. 5. In contrast to the poor correlation between the ρ_0 values and the Mo-complex concentration in the as-plated state, the resistivity of the heat treated Ni–Mo–P films increases with increasing Mo-complex concentration. Although no clear explanation is given for the ρ value variation of Mo codeposited Ni–P films, the molybdenum content plays one of the most important roles to determine the resistivity and the structure after heat treatment. Moreover, the codeposited molybdenum improves the thermal stability of resistivity, and it might be due to the fact that the codeposited molybdenum disturbes the structural change by heat treatment.

Conclusion

The characteristics of electroless Ni–Mo–P alloy films, which were prepared by addition of the Mo-complex into the bath, have been studied. The deposition rate and the phosphorus content decrease with increasing Mo-complex concentration. The structure of Ni–Mo–P alloy films is changed from amorphous to crystalline on increasing Mo-complex

concentration. X-Ray diffraction measurements indicate that codeposited Mo forms a solid solution with a Ni matrix. From DSC, X-ray diffraction and resistivity measurement, the Ni-Mo-P alloy film is thermally stabler than the Ni-P film. In general, a thin film resistor is actually used after heat treatment. The resistivity of the Ni-P film after heat treatment is changed abruptly by a structural transformation. Since the Ni-Mo-P films described in the text, show very stable resistivity against 400 °C heat treatment, electroless Ni-Mo-P alloy films have much advantage for the usage in thin film resistors. Under as-plated conditions, the correlation between resistivity and Mo content is not clear, however after heat treatment, the resistivity strongly depends on the Mo content, and the resistivity after heat treatment increases with increasing Mo content.

The authors wish to thank Professor Emeritus Dr. T. Yoshida, Waseda University, and Dr. K. Nihei and Mr. H. Sawai, the Research Labs, OKI Electric Industry Co. Ltd., for their encouragement of the work.

References

1) N. Miura, Y. Fuura, and A. Kazumi, *IEEE Trans. Components. Hybrids, Manuf. Technol.*, **CHMT-4**, 532 (1981).
2) J. Dearden, *Electrocomponent Sci. Technol.*, **3**, 103 (1976).
3) Y. Tokunaga, M. Yoshida, and M. Kizawa, *IEEE Trans. Components, Hybrids, Manuf. Technol.*, **CHMT-4**, 148 (1981).
4) N. Sinnadurai and K. J. Wilson, *IEEE Trans. Components, Hybrids, Manuf. Technol.*, **CHMT-5**, 308 (1982).
5) A. W. Goldstein, W. Rostoker, F. Schossberger, and G. Gutzeit, *J. Electrochem. Soc.*, **104**, 104 (1957).
6) J. P. Marton and M. Schlesinger, *J. Electrochem. Soc.*, **115**, 16 (1968).
7) P. J. Cote, *Solid State Commun.*, **18**, 1311 (1976).
8) A. H. Graham, R. W. Lindsay, and H. J. Read, *J. Electrochem. Soc.*, **109**, 1200 (1962).
9) A. H. Graham, R. W. Lindsay, and H. J. Read, *J. Electrochem. Soc.*, **112**, 401 (1965).
10) J. Diximer and K. Doi, *Compt. Rend.*, **257**, 2451 (1963).
11) B. G. Bagley and D. Turnbull, *J. Appl. Phys.*, **39**, 5681 (1968).
12) J.-P. Randin and H. E. Hinterman, *J. Electrochem. Soc.*, **115**, 480 (1968).
13) J.-P. Randin, P. A. Maire, E. Saurer, and H. E. Hintermann, *J. Electrochem. Soc.*, **114**, 442 (1967).
14) K. Masui, S. Maruno, and T. Yamada, *J. Jpn. Inst. Metals*, **41**, 1130 (1977).
15) K. Masui, M. Tachihara, T. Yamada, and T. Tsujimoto, *J. Jpn. Inst. Metals*, **44**, 124 (1980).
16) F. Pearlstein and R. F. Weightman, *Electrochem. Tech.*, **6**, 427 (1968).
17) K. Aoki and O. Takano, *Ex. Abstract the 58th Conf. of Metal Finishing Soc. Jpn.*, (1978), p. 52.
18) G. O. Mallory, *Plating and Surface Finishing*, **63**, No. 6, 34 (1976).
19) M. Schwartz and G. O. Mallory, *J. Electrochem. Soc.*, **123**, 606 (1976).
20) G. O. Mallory and T. R. Horhn, *Plating and Surface Finishing*, **66**, No. 4, 40 (1979).
21) L. G. Svendsen, T. Osaka, and H. Sawai, *J. Electrochem. Soc.*, **130**, 2252 (1983).
22) T. Osaka and I. Koiwa, *Kinzoku Hyomen Gijutsu*, **34**, 330 (1983).